EasyChair Preprint

№ 6781

Simulation of Lead Removal Using Palm Kernel Shell Activated Carbon in a Packed Bed Column

Rachel Fran Mansa, Ming Ling Ting, Audrey Osong Patrick and Sivakumar Kumaresan

October 6, 2021

SIMULATION OF LEAD REMOVAL USING PALM KERNEL SHELL ACTIVATED CARBON IN A PACKED BED COLUMN

Rachel Fran Mansa*, Ting Ming Ling, Audrey Osong Patrick, Sivakumar Kumaresan

Chemical Engineering Programme, Faculty of Engineering,
88400 Universiti Malaysia Sabah, Malaysia
*Corresponding Author: rfmansa@ums.edu.my

ABSTRACT. *The abundance and excellent adsorption efficiency of palm kernel shell activated carbon (PKSAC) made it a popular choice as a potential adsorbent for heavy metal removal from wastewater, especially lead (Pb^{2+}) generated by lead-based industry. However, the practicability of PKSAC is limited to the laboratory scale. This work focuses on dynamic simulation of Pb^{2+} adsorption by PKSAC packed bed column using Aspen Adsorption V10® to investigate the feasibility of PKSAC for industrial scale Pb^{2+} removal. The physical properties of PKSAC and equilibrium data of Pb^{2+} adsorption obtained from existing laboratory experiments were inserted into a liquid plug flow packed with a linear lumped resistance model. The column performance in terms of breakthrough, saturation, and adsorption capacity were evaluated and Average Relative Error (ARE) was applied to affirm the reliability of the data and model. Seven out of eight simulation runs showed agreeable results with literature works, where there were five runs that achieved ARE less than 0.05. Langmuir isotherm was found to be better fitted with chemisorption of Pb^{2+} onto chemically activated PKSAC, while Freundlich isotherm suitably described physisorption occurred on physically treated PKSAC. The adsorption efficiency was also found to be proportional to the bed diameter and height, and reverse with an increment of flowrate and Pb^{2+} concentration. The temperature did not show a significant effect on the column breakthrough and adsorption capacity. In comparison with other types of adsorbent material which reached breakthrough at 2.3h, the PKSAC packed bed column achieved a significantly longer breakpoint at 10^{th} days, under constant operational parameters and bed dimensions. To further optimize the column to control lead concentration from industrial effluent below 0.1 mg/L with 3 months service time, the packed bed was sized to 3.8 m height and 0.75 m diameter to treat effluent that contains 26 mg/L of Pb^{2+} at 100 m^3/day.*

KEYWORDS. Palm kernel shell activated carbon, lead adsorption, isotherm, dynamic simulation, scale-up.

INTRODUCTION

With the increase of industry and urbanized areas, untreated industrial effluents have increased and released into the environment (Kaushal & Singh, 2017). One of the critical pollutants is lead (Pb^{2+}), which is a type of heavy metal that is non-degradable and can be easily absorbed into the bloodstream if consumed. Major industrial wastewaters that contain Pb^{2+} are from the lead battery industry, coal oven effluent, metal mines, coal combustion, and electroplating industry, where the concentrations of Pb^{2+} range from 0.03 mg/L to as high as 25.39 mg/L (Jusoh *et al*., 2007). World Health Organization has advised that the drinking water must not contain more than 0.1 mg/L of Pb^{2+}, and the consumption of lead-contained water by humans should be below 1.75 mg/person/week (*World Health Organization*, 2011). Exceeded levels of Pb^{2+} intake can cause severe health problems such as nervous and reproductive system damages, anemia, hallucination, coma, and even death (Malakootian *et al*., 2009; Bali & Tlili, 2019). The United States Environmental Protection Agency (EPA) also advises that the lead content in wastewater must be reduced to not more than 0.15 mg/L prior to discharge (*UN Water*, n.d.). Therefore, the removal of Pb^{2+} from water is extremely important to meet international regulations and ensure a safer environment for human and aquatic lives.

Among a variety of water treatment technologies such as reverse osmosis, membrane filtration, ultrafiltration, ion-exchange, precipitation, coagulation, electrodialysis, and calorimetric. The

adsorption process has been found to be more favourable due to its higher efficiency, lower energy input, ease of use, technology readiness, and even reusable (Baby and Hussein, 2020). Packed bed column is generally used in the adsorption process, while activated carbon is used as an adsorbent in the purification of water from heavy metal contamination as it is cost-effective, environmental-friendly, and possesses extremely high adsorption capacity owing to its microporous structure (Marsh and Rodríguez-Reinoso, 2006).

Conventionally, activated carbon (AC) is produced from coal, coke, petroleum, wood, lignite, and peat, which are quite expensive and unsustainable. Derivation of biomass and agricultural waste into less expensive AC has become the trend (Rashidi and Yusup, 2018; Saleem *et al*., 2019). Palm kernel shell (PKS) is comparable to coconut shell, olive stone, grape stalk, bamboo, almond shell. This is due to the simple processing steps, sustainability and reproducibility (Baby and Hussein, 2020; Opoku *et al*., 2020), low cost, abundance, and excellent physical characteristics such as high volatility, specific area, pore-volume, carbon content (Geankoplis, 2003; Rugayah *et al*., 2014), and adsorption capacity (> 90 mg/g) (Saka *et al*., 2012). PKS was found to have a high affinity for Pb^{2+} due to the functional groups such as carboxyl, hydroxyl, and lactone on their graphite layers that can favourably attract positive-charge heavy metals (Sulaiman *et al*., 2011). Table 1 shows the physical characteristics and proximate analysis of raw PKS and PKSAC, where iodine number shown was the estimation of surface area of adsorbent, and their micrography are shown in Figure 1.

Table 1. Properties of raw PKS and PKSAC.

Analysis	Material & Author	Raw PKS	Steam-activated PKSAC	KOH-activated PKSAC
		(Rugayah *et al*., 2014)		Jawing *et al*., 2020
Physical properties	BET surface area (m^2/g)	0.7214	607.76	-
	Micropore surface area (m^2/g)	-	541.76	-
	Total pore volume (cm^3/g)	-	0.25	-
	Micropore volume (cm^3/g)	-	0.21	-
	H/C ratio	0.1065	0.05	-
	Iodine number (mg/g)	-	-	1209.27
Proximate analysis (wt %)	Moisture content	12.7	3.56	2
	Volatile compounds	61.7	10.81	-
	Fixed carbon	23	83.07	-
	Ashes	2.3	2.56	8

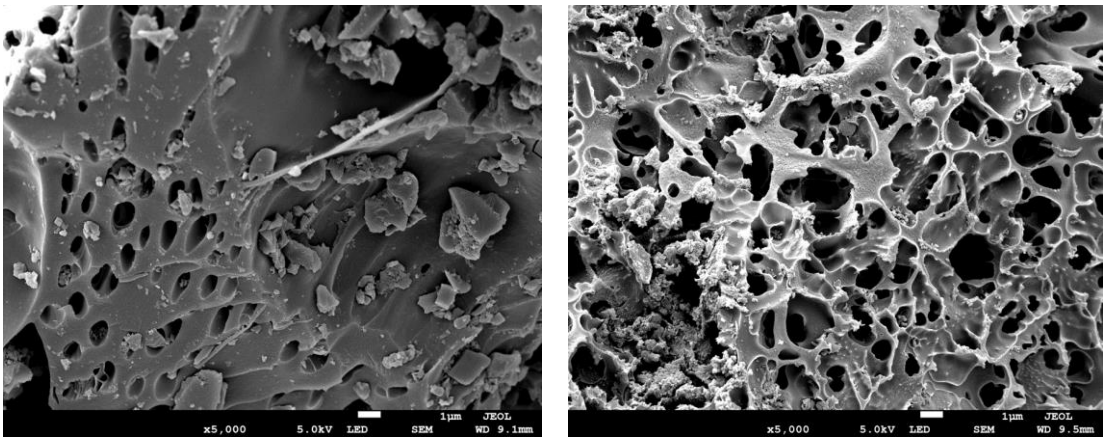

Figure 1. Field Emission Scanning electron microscopy (FESEM) micrograph of raw PKS (left) and KOH treated PKSAC (right) at magnification of 5000X. (Source: Jawing *et al*., 2020 paper in review)

Removal of lead ions through adsorption by PKSAC had been carried out by several researchers. However, the application of PKSAC in pilot or commercial scale packed bed adsorption systems for lead removal has not been reported to the best of our knowledge. Setting up a large-scale study requires more investment and time, in addition to the challenge of keeping certain variables constant for the evaluation of adsorption efficiency as a function of process parameters. Dynamic

simulation using Aspen Adsorption® is proposed to study the adsorption of Pb^{2+} by PKSAC without having to set up a cost- and time-consuming adsorption column. This study aims to simulate Pb^{2+} adsorption onto PKSAC in a packed bed column by using Aspen Adsorption® V10 to determine the adsorption efficiency of PKSAC in terms of adsorption capacity.

THEORETICAL MODELLING OF SIMULATION IN ASPEN ADSORPTION® V10

Momentum/Material Balance

The Ergun equation is generally used to explain the momentum balance in a packed bed column:

$$\frac{\partial c}{\partial t} + v_s \frac{\partial c}{\partial z} + \frac{1-\varepsilon_b}{\varepsilon_b} \rho_p \frac{\partial q}{\partial t} = D_L \frac{\partial^2 c}{\partial z^2} \qquad \textit{(Equation 1)}$$

where c is the concentration of the aqueous solution, q is adsorbate amount in the solid phase, $\frac{\partial q}{\partial t}$ is mass transfer rate, v_s is the superficial velocity of the solution $\left(\frac{m}{s}\right)$, ε_b is bed voidage, ρ_p is adsorbent particle density $\left(\frac{g}{m^3}\right)$, z is column length (m), and D_L is axial dispersion coefficient $\left(\frac{m^2}{s}\right)$. $\frac{\partial q}{\partial t}$ depends on the adsorption mechanism such as external diffusion, internal diffusion, and surface reaction.

External diffusion is also known as interphase or film diffusion, where the solute is transported from its bulk solution to the surface area of the adsorbent. Internal diffusion is the second stage of transport where the solute moves from the external surface of the adsorbent to its pores. Lastly, surface reaction refers to a physical or chemical reaction where the solutes are simultaneously adsorbed and desorbed at the internal surfaces of the adsorbent until both sorption rates are equal and equilibrium is achieved (Tien, 2019). These mass transfer mechanisms greatly depend on the adsorbent pore size and pore distributions, the molecular size of adsorbates, as well as process parameters such as flow rate, concentration, temperature, pH, and contact time. Among the three adsorption steps, the one that contributes the largest mass transfer resistance is known to be the rate-controlling or rate-limiting step which will determine the effective rate of adsorption (Wang *et al.*, 2020).

Kinetic Modelling

Kinetic models such as pseudo-first-order (PFO) and pseudo-second-order (PSO) kinetic models have been popularly used to examine the reactive adsorption behaviour and rate of heavy metals towards adsorbents. For simplicity, the linear lumped resistance model is generally used where all the mass transfer driving forces in adsorption including surface reaction and diffusion resistances are lumped into a constant mass transfer coefficient (MTC), which acts as a linear function of the adsorbent loading. The overall adsorption rate of Pb^{2+} onto PKSAC can be defined as:

$$\frac{1}{K_i} = \frac{R_p}{3k_{fi}} + \frac{R_p^2}{15\varepsilon_p D_p} \qquad \textit{(Equation 2)}$$

where K_i is the global MTC (1/s), R_p is adsorbent particle radius (m), D_p is the pore diffusion coefficient (m^2/s), and ε_p is the adsorbent porosity. k_{fi} is external MTC (m/s) that correlated to dimensionless groups: Sherwood (Sh), Reynolds (Re), and Schmidt (Sc) (Wilson and Geankoplis, 1966):

$$Sh = \frac{d_p \cdot k_{fi}}{D_m} = 2 + 1.1 Sc^{\frac{1}{3}} Re^{0.6} \qquad \textit{(Equation 3)}$$

The Reynolds and Schmidt number can be calculated as equation shown below:

$$Re = \frac{\rho_f v_s d_p}{\mu} \qquad \textit{(Equation 4)}$$

$$Sc = \frac{\mu}{\rho D_m} \qquad \textit{(Equation 5)}$$

ρ_f and μ refer to density (kg/m^3) and dynamic viscosity (kg/ms) of the fluid, respectively. d_p is the adsorbent particle diameter (m). D_m (m^2/s) is the molecular diffusivity which can be represented as:

$$D_m = 2.74 \times 10^{-9} (M_f)^{1/3} \qquad \textit{(Equation 6)}$$

where M_f is the molecular weight (kg/kmol) of the fluid. The correlation of pore diffusion, D_p (m^2/s), Knudsen diffusion, D_k (m^2/s), molecular diffusion, D_m (m^2/s), and particle tortuosity, τ_p is expressed as:

$$\frac{1}{D_p} = \tau_p \left(\frac{1}{D_m} + \frac{1}{D_k}\right) \quad \textit{(Equation 7)}$$

$$D_k = 97 r_p \left(\frac{T}{M_f}\right)^{0.5} \quad \textit{(Equation 8)}$$

$$\tau_p = \varepsilon_p + 1.5(1 - \varepsilon_p) \quad \textit{(Equation 9)}$$

where r_p is the adsorbent pore radius and T is the solution temperature.

Adsorption Isotherms

Adsorption of Pb^{2+} onto PKSAC has been mostly studied by using Langmuir and Freundlich isotherms. The Langmuir isotherm is formulated based on a kinetic principle which assumes that (1) the rate of adsorption onto a solid surface is equal to the rate of desorption from the solid surface where the adsorption activation energy and molecules enthalpies are constant at all sites, (2) it is monolayer adsorption occurred at an identical and finite number of active sites, where all sites of adsorbents have an equal affinity towards the adsorbates, and (3) there is negligible interaction between the adsorbate molecules (Langmuir, 1916; Latour, 2015). The Langmuir isotherm has the following equation:

$$q_e = \frac{q_m \cdot K_L \cdot C_e}{1 + K_L \cdot C_e} \quad \textit{(Equation 10)}$$

where q_e represents the adsorption capacity (mg/g) at equilibrium, q_m is the theoretical maximum amount of adsorbates that attach to one unit mass of adsorbent to form a monolayer, and K_L is Langmuir constant (L/mg).

The Freundlich isotherm is an empirical model that assumes a non-uniform distribution of heat and affinities, and possibly multilayer adsorption over a heterogeneous surface of adsorbent (Ho, 2006). The stronger binding sites will be occupied first, and the adsorption energy will decrease exponentially with increasing occupied sites (Setiabudi *et al*., 2016). The non-linear equation of Freundlich isotherm is shown:

$$q_e = K_F C_e^{\frac{1}{n}} \quad \textit{(Equation 11)}$$

where K_F is the Freundlich constant [(mg/g)(L/mg)$^{1/n}$] that relates to the adsorption capacity, and $1/n$ refers to the surface heterogeneity or the adsorption intensity.

The assessment of the fitness of mathematical models to the experimental data in an adsorption process uses error function analysis, where the deviation of adsorption capacity between actual experimental data and model value is calculated (Sarici-Özdemir and Önal, 2013). Two assessments of fitness were used in this study, the coefficient of determination (R^2) and the average relative error (ARE). The model with an R^2 value of more than 0.9 and closest to 1 indicates a higher degree of fitness to the experimental data. ARE calculates the difference of adsorption capacity between actual experimental data and simulated or mathematically modeled data (Kapoor and Yang, 1989).

$$ARE = \sum_{i=1}^{N} \left[\frac{q_{e(exp)} - q_{e(cal)}}{q_{e(exp)}}\right]_i \quad \textit{(Equation 12)}$$

If ARE ≤ 0.05, it indicates that the results could be highly consistent. If ARE < 0.1, the data is probably consistent. If ARE > 0.1, the result is inconsistent.

Column Breakthrough and Scale-up

The breakthrough curve is a useful plot that can help to determine the column breakthrough time (t_b) and saturation time (t_{st}), which are usually set at 5 and 95 % of initial concentration ($0.05C_o$ & $0.95C_o$), respectively (Geankoplis, 2003). Generally, breakthrough time is a linear function of adsorption capacity, which is the measurement for adsorbent performance and adsorption efficiency of an industrial packed bed column. The capital and operating costs of an adsorption process are highly subjected to the column service time and exhaustion rate when the feed flow rate, solute concentration, and adsorbent characteristics are constant (McKay, 1996; Nassar *et al*., 2003). When the adsorption capacity of adsorbent used is low, the amount of adsorbate that can be held by the adsorbent is limited, thus leading

to a fast column breakthrough and short operating or service time, which then incurs additional labour cost for frequent changing of adsorber bed. Therefore, an adsorbent that has high adsorption capacity is preferable to prolong the service time of an adsorber (Iheanacho *et al*., 2021).

The volume of effluent treated (V_b), the total amount of Pb^{2+} adsorbed (q_{total}), and the adsorption capacity of PKSAC (q_e) can be calculated by using the following formula (Juela, 2020):

$$V_b\ (m^3) = Q \times t_{st} \qquad \textit{(Equation 13)}$$

$$q_{total}\ (mg) = \left(Q \int_{t=0}^{t=t_{st}} c_R\ dt \right) \qquad \textit{(Equation 14)}$$

$$q_e \left(\frac{mg}{g}\right) = \frac{q_{total}}{m} \qquad \textit{(Equation 15)}$$

where c_R is the concentration of Pb^{2+} adsorbed and m is the mass of PKSAC used in the column. This information is useful for column bed design for a particular amount of lead-enriched wastewater and service time. Length of unused bed (LUB) proposed by Collins (1967) is popularly used to determine the bed length (capacity) that has not been saturated at the breakpoint:

$$LUB = \left(1 - \frac{q_b}{q_e}\right) L = L_T - L_B = L_T - \frac{t_b}{t_{st}} L_T \qquad \textit{(Equation 16)}$$

where q_b is the adsorption capacity at a breakpoint, L is the length of the column, L_{UNB} is unused bed length, which also represents the remaining available mass transfer zone (MTZ) of the column. The ratio t_b/t_{st} is also equivalent to L_B/L_T which is the fraction of the total bed capacity that can be utilized up to breakpoint.

METHODOLOGY

Research Chronology

Aspen Adsorption® V10 was used to carry out the dynamic simulation of Pb^{2+} removal by PKSAC. Simulation trials were conducted based on past experimental works that used PKSAC as adsorbent and Pb^{2+} as adsorbate, with the presence of equilibrium data. The simulation input data is shown in Table 3.

Table 3. Simulation input data.

Run	1	2	3	4	5	6	7	8
Author / Parameter	Baby & Hussein (2020)	Baby *et al*. (2019)	Akaangee *et al*. (2018)	Yi *et al*. (2016)	Nwabanne & Igbokwe (2012)	Oluyemi *et al*. (2012)	Onundi *et al*. (2010)	Issabayeva *et al*. (2006)
Q	1.2×10^{-6}	9.8×10^{-7}	6.2×10^{-7}	4.5×10^{-7}	2.7×10^{-6}	5.5×10^{-6}	2.1×10^{-6}	2.8×10^{-7}
C_0	7.6×10^{-5}	7.6×10^{-5}	4.5×10^{-4}	6.0×10^{-4}	2.3×10^{-3}	3.0×10^{-4}	4.5×10^{-6}	2.1×10^{-3}
T	27	27	25	25	30	25	25	27
Hb	0.011	0.01	0.015	0.005	0.015	0.0055	0.011	0.015
Db	0.0072	0.0066	0.007	0.0034	0.01	0.0036	0.0072	0.001
Ei	0.38	0.38	0.38	0.391	0.395	0.392	0.404	0.391
Rp	0.2125	0.225	0.1125	0.575	0.55	1.2	1.015	0.45
SFac	1	1	1	1	1	1	1	1
RHOs	680	680	680	680	680	680	680	680
MTC	0.60033	0.5591	1.9818	0.08942	0.09742	0.02177	0.03044	0.11505
$IP_{1,\ Langmuir}$	1.53382	14.9819	31.4019	29.6038	60.3865	12.4668	2.5393	28.744
$IP_{2,\ Langmuir}$	0.03312	5.8622	0.8611	2.48731	0.4246	0.43983	0.0266	3.7094
$IP_{1,\ Freundlich}$	0.3312	0.1457	4.0489	19.9018	10.4735	76.653	37.0944	-
$IP_{2,\ Freundlich}$	3.26797	1.0417	0.2144	0.10800	0.9980	0.4079	0.1186	-

**Note: Q= Flow rate (m^3/s), C_0=Concentration ($kmol/m^3$), T= Temperature (°C), Hb= Bed Height (m), Db= Bed diameter (m), Ei=Bed voidage (m^3 void/m^3 bed), Rp=Adsorbent radius (mm), SFac=Shape factor, RHO= Adsorbent density (kg/m^3), MTC=Mass transfer coefficient (s^{-1}), IP=Isotherm parameter*

Model Configurations and Specifications of Packed Bed Column

Table 4 shows the mathematical model selections and specifications for each simulation run.

Table 4. Configuration of adsorption model.

Configuration	Model Assumption	Configuration	Model Assumption
Discretization Method	Upwind Differencing Scheme 1	Kinetic Model	Linear Lumped Resistance
Material / Momentum Balance	Convection with Estimated Dispersion	Form of Mass Transfer Coefficient	Constant
Pressure Drop	None	Isotherm Model	Langmuir / Freundlich
Velocity	Constant	Energy Balance	Isothermal
Film Model	Solid		

For simulation of the laboratory scale data, the pressure drop is neglected, and velocity is assumed to be constant. The adsorption system is also assumed as isothermal due to the lack of thermodynamic data. The column height and diameter, bed porosity, adsorbents' radius, shape factor, and density, as well as isotherm parameters, were determined based on literature and correlation study. Some unavailable data such as adsorbent size, shape factor, density, and bed voidage were acquired from relevant and correlation studies (Mak *et al*., 2009; Chen *et al*., 2012; Evbuomwan *et al*., 2013; Benyahia and O'Neill, 2005).

Simulation Run and Result Analysis

For each set of a simulation run, a graph was created by clicking "New Form", where the x-axis was time profile by default, and the y-axis was set as the outlet concentration of Pb^{2+}. The simulation was started and let run until Pb^{2+} adsorption reached saturation. By right-clicking the graph and selecting "Show as history", time-concentration data were shown. These data were copied to Microsoft Excel and breakthrough analyses were carried out. t_b, t_{sat}, V_b, q_{total}, and q_e were also determined. The simulation run was then repeated by using different isotherm data, and the results were compared and validated via ARE.

Effects of Parameters

The simulation runs that achieved ARE less than 0.05, with considerable adsorption capacity and high R^2 (from original works), were selected for subsequent simulation trials and scale-up design. Trials were made to investigate the effect of varying parameters such as fluid flow rate, solute concentration, bed diameter, and bed height. Parameters were altered one at a time within 20% deviation from the original value while keeping the other properties constant.

Feasibility and Scale-up of Column

The feasibility of the PKSAC packed bed column was validated by comparing its breakthrough time (t_b) to the other similar existing work, as t_b is proportional to the adsorption capacity and service time. The column dimensions and process parameters were synchronized to that of the lead adsorption study carried out by Ronda *et al*., (2018), who used olive tree pruning biosorbent. The data is presented in Table 5.

Table 5. Scale-up data of the PKSAC packed bed column based on the parameters provided in the work done by Ronda *et al*., 2018.

Parameters	Value	Parameters	Value
Bed height	2.26 m	Flow rate	5333.4 L/h
Bed diameter	0.5 m	Linear velocity	0.00755 m/s
Bed height/diameter ratio	4.52	Space velocity	0.003 s^{-1}
Adsorbent mass	148.5 kg	Residence time	300 s
Temperature	25 °C	Pb^{2+} concentration	100 mg/L

After the verification of the PKSAC feasibility for Pb^{2+} removal, the simulation run was repeated by changing Pb^{2+} concentration to 26 mg/L, which is the maximum concentration found in the electroplating industry effluent (Jusoh *et al*., 2007). The bed diameter was also adjusted to 0.75 m, in order to reduce the discrepancy of the ratio of bed length and diameter (L/D) when the column is further scaled up. The other parameters such as flow rate, temperature, bed height, bed porosity, adsorbent density, sizes, and shape factor, as well as the isotherm parameters remained constant. The breakpoint concentration (c_b) was set at 0.1 mg/L, which is the upper limit value set by international standards. The breakthrough profile was observed, and the column height was then further optimized for three-month service by using LUB method.

RESULT AND DISCUSSION

Isotherm Analysis

The simulation result was tabulated in Table 6. The simulation run that gave the least ARE indicated a higher reliability of respective equilibrium data. The table also included coefficient of determination (R^2) obtained from corresponding literature as well as PKSAC preparation method and physical characteristics. Based on the simulation results, Run 3, 4, 5, 7, and 8 were better fitted to the Langmuir isotherm, while Run 1, 2, and 6 were more suitably described by the Freundlich isotherm.

Table 6. Simulation result.

Run	Iso.	t_b (s)	t_{st} (s)	V_b (m^3)	q_{total} (mg)	q_e (mg/g)	$q_{e,lit.}$ (mg/g)	ARE	R^2, lit	Prep. Method
1	L	110	440	5.16×10^{-4}	0.728	36.4	50	0.27	0.9548	H_3PO_4, 500 - 900°C
	F	170	560	6.57×10^{-4}	0.987	49.4		0.01	0.9993	
2	L	80	360	3.53×10^{-3}	0.478	32.4	49.64	0.35	0.23	Physical treatment
	F	80	340	3.33×10^{-3}	0.464	31.6		0.36	0.943	
3	L	420	980	6.12×10^{-3}	6.29	105.0	107.2	0.02	0.9982	H_3PO_4 + EDTA, 600°C
	F	430	820	4.73×10^{-3}	5.66	94.4		0.12	0.9673	
4	L	310	2930	1.32×10^{-4}	1.710	85.6	98	0.13	0.999	Source: Guoqing Water Purification Material Co. Ltd. (China)
	F	230	1940	8.73×10^{-5}	1.175	58.7		0.40	0.518	
5	L	1400	7000	2.09×10^{-3}	7.956	180.85	200	0.09	0.986	H_3PO_4, 800°C
	F	1400	6900	1.87×10^{-3}	7.242	176.63		0.12	0.976	
6	L	130	2490	1.36×10^{-4}	0.505	50.47	74.08	0.32	0.8212	Physical treatment
	F	370	3360	1.84×10^{-4}	0.763	76.3		0.03	0.9653	
7	L	40	1180	2.50×10^{-3}	0.136	1.36	1.337	0.02	0.978	Source: KD Technology (Malaysia)
	F	70	1080	2.29×10^{-3}	0.135	1.35		0.01	0.709	
8	L	200	900	1.89×10^{-3}	0.908	90.8	95.2	0.05	0.99	Source: Pacific Activated Carbon (Malaysia)

The Langmuir isotherm was fitted into Run 3 and 5, where the PKSAC in both experiments were prepared via chemical activation, and they had adsorption capacity of 107.2 and 200 mg/g

(Akaangee *et al*., 2018; Nwabanne & Igbokwe, 2012), respectively. The high adsorption capacity could be attributed to the PKSAC preparation method by using H_3PO_4, which is a type of acidic chemical that can effectively minimize the formation of tar that could inhibit the development of AC porous structure. After carbonization, the hydrated H_3PO_4 in salt form occupied in the AC pores can be washed away, resulting in PKSAC with more micropores and mesopores, therefore increasing the specific surface area and pore volume (Ulfah *et al*., 2019). This has also directly enhanced the adsorption capacity of PKSAC (Asnawi *et al*., 2019).

Naturally, PKSAC has surface functional groups such as carboxyl, hydroxyl, and lactone that have negative charges and tend to attract positively charged metal components (Sabzehmeidani *et al*., 2021; Sulaiman *et al*., 2011). For instance, the deprotonated carboxylic group may interact with Pb^{2+} cations via electrostatic interaction or ion exchange, and the aromatic compounds on PKSAC surface could form π-cation with Pb^{2+} (Deliyanni *et al*., 2012; Shi *et al*., 2018). Chemical activation methods could further enrich the functional groups on PKSAC surface, therefore increasing the metallic affinity and adsorption efficiency (Asnawi *et al*., 2019). This explains the fitness of Langmuir isotherm to the chemically activated PKSAC as the adsorbent has more homogeneous adsorptive sites with equal energy distribution, causing all the attached molecules fixed at finite active sites and resulting in monolayer coverage on PKSAC (Akaangee *et al*., 2018). Based on the review by Gao *et al*. (2020), the most efficient acidic and alkaline activating agents are KOH and H_3PO_4, respectively. Neutral activating agents such as zinc chloride ($ZnCl_2$), iron chloride ($FeCl_3$), and potassium carbonate (K_2CO_3) could also yield AC with significant specific surface area and total pore volume.

The Langmuir isotherm was also fitted to Run 4, 7, and 8, where the PKSAC were purchased and readily being used. These adsorbents also had very high surface area and pore volume, which may indicate that they were chemically activated. According to the literature data, R^2 values of Freundlich isotherm in Run 4 and 7 were 0.518 and 0.709, respectively. Both of the values were significantly lower than 0.9. In contrast, The Langmuir isotherm had R^2 of 0.999, 0.978, and 0.99, respectively in Run 4, 7, and 8. Therefore, it was further ascertained that chemisorption occurred in the chemically activated PKSAC adsorption system.

The Freundlich isotherm was fitted to Run 2 and 6, where the PKSAC were prepared through physical treatment. Freundlich isotherm is used to describe a physisorption where adsorbate and adsorbent interact via weak electric charges such as London forces, dipole-dipole forces, and Van der Waals. As this is a reversible process, adsorbate molecules attach to the heterogenous adsorbent surface freely and form a multilayer of adsorbates. Besides, R^2 values of Langmuir isotherm for Run 2 and 6 determined from literature work were 0.23 and 0.8212, respectively. These values were relatively low compared to that of Freundlich isotherm which recorded 0.943 and 0.9653. This indicates that Freundlich isotherm is more suitable to describe an Pb^{2+} adsorption system that employs physically treated AC.

Run 1 was found to be better fitted to Freundlich isotherm, despite the chemical activation of the PKSAC. Nevertheless, Langmuir isotherm had R^2 of 0.9548, which also indicated a favourable adsorption. This could tell that part of the system was physisorption, and another part was dominated by chemisorption, where at least half of adsorbent surfaces were heterogeneous and covered by multiple layers of adsorbates (Wang and Guo, 2020).

From the results, the adsorption of Pb^{2+} onto PKSAC could be due to either physisorption or chemisorption, depending on the adsorbent preparation method, and probably the operating conditions such as pH value of solution (ul Haq *et al*., 2017). In general, chemical-activated PKSAC tends to have chemisorption and better fitted by Langmuir isotherm, while physically treated PKSAC results in physisorption and suitably modelled by Freundlich isotherm. Nevertheless, chemical activation is more advantageous to effectively increase specific surface area and porosity of PKSAC, as well as improve the adsorption affinity of PKSAC towards heavy metals (Liu *et al*., 2020; Khedr *et al*., 2014).

Effect of Concentration

From Figure 2(a), the manipulation of C_0 from 4.53×10^{-4} kmol/m^3 in 20% deviation showed no visible changes on the breakthrough time. This could be due to the very low concentration of Pb^{2+} in the solution that caused an insignificant effect to the adsorption system. For a diluted solution that has high affinity towards adsorbent, external diffusion, where Pb^{2+} from bulk solution moves to the external surface of PKSAC through liquid film, is found to be more profound. Whereas, internal diffusion which

refers to the transportation of Pb^{2+} from PKSAC surface into the adsorbent pores, governs an adsorption system that has high solute concentration with low affinity towards adsorbent (Wang *et al*., 2020). Theoretically, adsorbents will get saturated sooner when the solute concentration increases, as the binding sites of adsorbents are occupied sooner by the greater amount of adsorbates per unit time (Chowdhury *et al*., 2013). At higher adsorbate concentration, larger driving forces are exerted which decreases the liquid film thickness and overcome the mass transfer resistances (Tien, 1994). Therefore, external diffusion rate is accelerated and Pb^{2+} ions could easily bind to the active sites on PKSAC (Ali *et al*., 2016; Moreno-Piraján *et al*., 2008).

Effect of Flowrate

The breakthrough curve plotted in Figure 2(b) indicates that the bed reached breakthrough earlier at 320 s, when the flowrate was 20% increase from 6.235×10^{-7} m^3/s to 7.482×10^{-7} m^3/s. In contrary, 20% reduction of initial flow rate to 4.988×10^{-7} m^3/s resulted in a later breakthrough at 480 s. This trend was found similar to other Pb^{2+} adsorption studies (Patel, 2020; Yahya *et al*., 2020; Alexander *et al*, 2017).

Despite a higher flow rate introduces larger amounts of effluent into the column per unit time, it also increases the mass transfer rate and decreases mass transfer resistance, therefore reducing the residence time and diffusivity of Pb^{2+} in the column bed. This directly leads to an earlier equilibrium state and column breakthrough, but the adsorption uptake is also relatively low, which indicates a lower adsorption efficiency (Yi *et al*., 2016). To effectively remove Pb^{2+} and improve adsorption capacity of the packed bed column for a relatively high flow rate, it is suggested to increase the column bed height and/or diameter to allow a reasonable residence time, which usually ranges between 10 to 60 minutes (Kopsidas, 2016; Cooney, 1998).

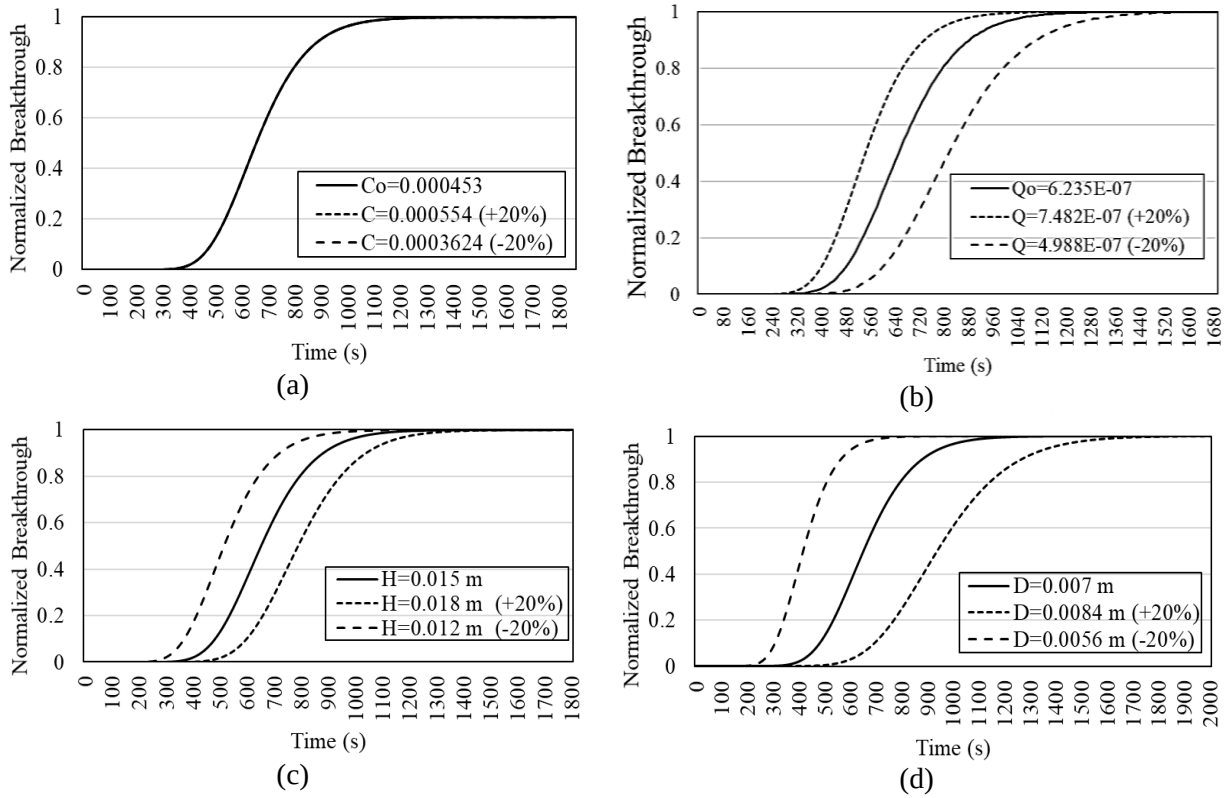

Figure 2. Breakthrough curve analyses at varying parameters: (a) concentration, (b) flowrate, (c) bed height, and (d) bed diameter.

Effect of Bed Height

The adsorption column bed height was found to have significant effect on column breakthrough. Figure 2(c) shows that the bed height with shorter length (0.12m) had the fastest breakthrough at 350 seconds with the steepest curve slope, while the greatest bed height (0.18m) achieved a longer breakthrough time at 520 seconds with the least steep curve. Similar tendency has been found in the other work

(Sizirici and Yildiz, 2020; Ghani and Jami, 2020; Biswas and Mishra, 2015). This is because a longer bed with fixed depth has more adsorbents which provide more active sites for adsorbing Pb^{2+}. Therefore, the mass transfer zone increases, and more contact time is allowed for the Pb^{2+} to diffuse into adsorptive sites until the adsorbent bed reaches equilibrium state (Patel, 2019). This also has also directly increased the adsorption capacity of the column. Therefore, column bed height plays a significant role in scale-up design in order to achieve a high adsorption capacity and lengthen the service time of a packed bed column of about three to four months with efficient Pb^{2+} removal.

Effect of Bed Diameter

The breakthrough curve plotted in Figure 2(d) shows that, at the smallest bed diameter of 0.034 m, breakpoint occurred at about 300 seconds, while the largest diameter of 0.051 m achieved a longer breakthrough time which is about 590 seconds. The effect of bed diameter is similar to that of bed height, where increasing the bed diameter would result in a longer breakthrough time. This is because a larger bed diameter allows more adsorptive sites as well as residence time. Consequently, the adsorption capacity increases and takes more time to reach equilibrium state, which also indicates that more Pb^{2+} can be removed from the effluent. Therefore, the scale-up design of the packed bed column shall consider a larger bed diameter for effective Pb^{2+} removal with desired service time of about three to four months.

Feasibility of PKSAC Packed Bed Column

Figure 3(a) shows the breakthrough curve from the work by Ronda *et al*. (2018) using olive tree pruning biosorbent, while Figure 3(b) depicts the breakthrough curve simulated in this work. At constant bed size and process conditions, the adsorption system using PKSAC reached breakthrough at 10^{th} day, which was far longer than that of biosorbent that had breakthrough time at 140 min or 2.3 h. The adsorption capacity of PKSAC was also found to slightly increase from 103 mg/g in laboratory study to 113 mg/g in industrial scale. This further ascertains that PKSAC is excellent adsorbent with great adsorption capacity and able to treat more amounts of lead polluted wastewater.

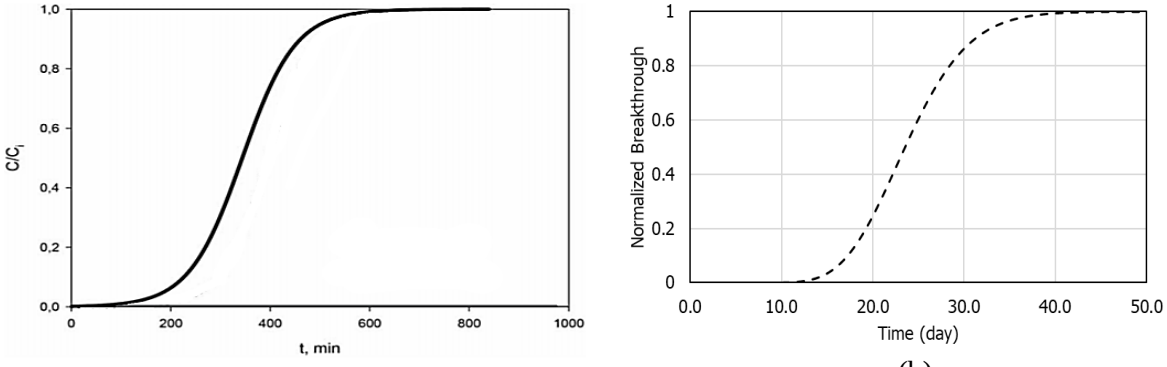

(a) (b)

Figure 3. Comparison of breakthrough curves of Pb^{2+} adsorption by (a) using olive tree pruning biosorbent (Ronda *et al*.,2018), and (b) PKSAC at constant bed dimensions and process parameters.

Scale-up of PKSAC Packed Bed Column

The concentration of the feed was further increased to 26 mg/L, which was the maximum Pb^{2+} concentration found in electroplating industry effluent (Jusoh *et al*., 2007). The breakthrough happened at 37.5 day, or 3.24×10^6 seconds. To lengthen the service time of the column to three months, or equivalent to 7.776×10^6 seconds, the bed height was optimized by using LUB method. The new bed length was found to be 3.8 m.

Figure 4 shows the new breakthrough curve which indicated that the scaled-up adsorption system reached breakthrough at 94.9th day. This means that the PKSAC packed bed column can effectively remove Pb^{2+} for three months. This would require approximately 805.8 kg of PSAC in the packed bed column, and 61.12 kmol of Pb^{2+} are being removed, The finalized scale-up data of PKSAC packed bed column for Pb^{2+} adsorption was shown in Table 7.

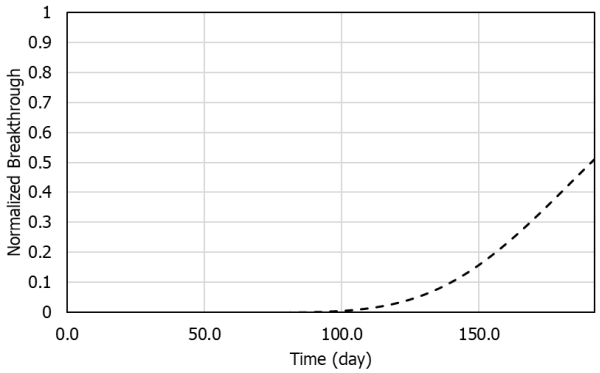

Figure 4. Breakthrough curve of industrial-scale PKSAC packed bed column designed for Pb^{2+} removal with three-month service time.

Table 7. Scale-up data of PKSAC packed bed column for electroplating industry effluent with three months service time.

Parameters	Values	Parameters	Values
Flow rate (m^3/day)	100	SFac	1
Concentration, C_0 (mg/L)	26	RHOs (kg/m^3)	640
Temperature (°C)	25	MTC (s^{-1})	0.0005692
Bed height (m)	3.8	Linear velocity (m/s)	0.0262
Bed diameter (m)	0.75	Space velocity (s^{-1})	0.0069
Adsorbent mass (kg)	805.8	Residence time (min)	24.17
Ei (m^3 void/m^3 bed)	0.38	$IP_{1,\ lead\ solution}$ (kmol/kg)	34.4448
Rp (mm)	0.2125	$IP_{2,\ lead\ solution}$ (m^3/kmol)	0.785024

CONCLUSION

Simulation of Pb^{2+} adsorption onto PKSAC packed bed column had been carried out in dynamic mode, where the data were based on previous studies. According to the simulation result and verified with experimental data, adsorption of Pb^{2+} onto chemically treated PKSAC was mostly described by the Langmuir isotherm, while the Freundlich isotherm better fitted with physisorption that occurred on physically treated PKSAC. The overall adsorption studies showed that chemical activation of PKSAC resulted in higher adsorption capacity and improved metallic affinity towards Pb^{2+}. In addition, the adsorption efficiency of the PKSAC packed bed column in terms of adsorption capacity and breakthrough time increased significantly with the increments of bed height and bed diameter and greatly declined when the flowrate and concentration increased.

The efficiency of PKSAC was ascertained when the column was scaled up and operated under the same conditions as other studies that used different types of adsorbents, where the PKSAC packed bed column was able to achieve breakthrough time at 10 days. By using the LUB Method, PKSAC packed bed column was scaled up to 3.8 m height and 0.75 m diameter in order to treat the effluent from the electroplating industry at 100 m^3/day which contains 26 mg/L of Pb^{2+}. The column was able to effectively adsorb Pb^{2+} for about 95 days with residence time of 24 minutes, ensuring the treated effluent less than 0.1 mg/L of Pb^{2+}. In the nutshell, commercial-sized PKSAC packed bed columns are feasible for Pb^{2+} removal from industrial effluent. PKSAC is reusable, biodegradable and a low-cost material which compensate for the additional processing cost of transforming agricultural waste into adsorbents.

REFERENCE

Akaangee, P. A., Halim Abdullah, A., Yen Ping, T., & Zainal, Z. (2018). Batch and Fixed Bed Adsorption of Pb(II) from Aqueous Solution using EDTA Modified Activated Carbon Derived from Palm Kernel Shell. In *BioResources* (Vol. 13, Issue 1).

Alexander, J. A., Surajudeen, A., Aliyu, E. N. U., Omeiza, A. U., & Zaini, M. A. A. (2017). Multi-metals column adsorption of lead (II), cadmium (II) and manganese (II) onto natural bentonite clay. *Water Science and Technology*, **76** (**8**), 2232-2241.

Ali, R. M., Hamad, H. A., Hussein, M. M., & Malash, G. F. (2016). Potential of using green adsorbent of heavy metal removal from aqueous solutions: Adsorption kinetics, isotherm, thermodynamic, mechanism and economic analysis. *Ecological Engineering*, **91**, 317–332.

Asnawi, T. M., Husin, H., Adisalamun, A., Rinaldi, W., Zaki, M., & Hasfita, F. (2019, June). Activated carbons from palm kernels shells prepared by physical and chemical activation for copper removal from aqueous solution. In *IOP Conference Series: Materials Science and Engineering*, **543** (**1**), p012096.

Baby, R., & Hussein, M. Z. (2020). Ecofriendly approach for treatment of heavy-metal-contaminated water using activated carbon of kernel shell of oil palm. *Materials*, **13** (**11**).

Baby, R., Saifullah, B., & Hussein, M. Z. (2019). Palm Kernel Shell as an effective adsorbent for the treatment of heavy metal contaminated water. *Scientific Reports*, **9** (**1**).

Bali, M., & Tlili, H. (2019). Removal of heavy metals from wastewater using infiltration-percolation process and adsorption on activated carbon. *International Journal of Environmental Science and Technology*, **16** (**1**), 249–258.

Biswas, S., & Mishra, U. (2015). Continuous fixed-bed column study and adsorption modeling: removal of lead ion from aqueous solution by charcoal originated from chemical carbonization of rubber wood sawdust. *Journal of Chemistry*, *2015*.

Chowdhury, Z. Z., Zain, S. M., Rashid, A. K., Rafique, R. F., & Khalid, K. (2013). Breakthrough curve analysis for column dynamics sorption of Mn (II) ions from wastewater by using Mangostana garcinia peel-based granular-activated carbon. *Journal of Chemistry*, *2013*.

Collins, J. J. (1967). The LUB/equilibrium section concept for fixed-bed adsorption. In *Chem. Eng. Prog. Symp. Ser* (Vol. 63, No. 74, pp. 31-35).

Deliyanni, E., Arabatzidou, A., Tzoupanos, N., & Matis, K. A. (2012). Adsorption of Pb2+ using mesoporous activated carbon and its effects on surface modifications. *Adsorption Science & Technology*, **30** (**7**), 627-645.

Gao, Y., Yue, Q., Gao, B., & Li, A. (2020). Insight into activated carbon from different kinds of chemical activating agents: A review. *Science of the Total Environment*, 141094.

Geankoplis, C. J., Hersel, A. A., & Lepek, D. H. (2018). *Transport processes and separation process principles* (Vol. 4). Boston, MA: Prentice hall.

Ghani, N. R. N. A., & Jami, M. S. (2020). Dynamic Adsorption of Lead by Novel Graphene Oxide-polyethersulfone Nanocomposite Membrane in Fixed-bed Column. *Journal of Advanced Research in Experimental Fluid Mechanics and Heat Transfer*, **2** (**1**), 1-9.

Ho, Y. S. (2006). Second-order kinetic model for the sorption of cadmium onto tree fern: A comparison of linear and non-linear methods. *Water Research*, **40** (**1**), 119–125.

Iheanacho, O. C., Nwabanne, J. T., Obi, C. C., & Onu, C. E. (2021). Packed bed column adsorption of phenol onto corn cob activated carbon: linear and nonlinear kinetics modeling. *South African Journal of Chemical Engineering*, **36**, 80-93.

Issabayeva, G., Aroua, M. K., & Sulaiman, N. M. N. (2006). Removal of lead from aqueous solutions on palm shell activated carbon. *Bioresource Technology*, **97** (**18**), 2350–2355.

Jawing, D., Syahril, S., Bahrun, M. H. V., & Mansa, R. F. (2020). Palm kernel shell activated carbon for lead and methylene blue removal. *Transactions on Science and Technology*, Vol. 6 (3).

Juela, D. M. (2020). Comparison of the adsorption capacity of acetaminophen on sugarcane bagasse and corn cob by dynamic simulation. *Sustainable Environment Research*, **30** (**1**), 1-13.

Jusoh, A., Su Shiung, L., Ali, N., & Noor, M. J. M. M. (2007). A simulation study of the removal efficiency of granular activated carbon on cadmium and lead. *Desalination*, **206** (**1**–**3**), 9–16.

Kapoor, A., & Yang, R. T. (1989). Correlation of equilibrium adsorption data of condensible vapours on porous adsorbents. *Gas Separation & Purification*, *3*(4), 187-192.

Kaushal, A., & Singh, S. (2017). Adsorption Phenomenon and its Application in Removal of Lead from Wastewater: A Review. *International Journal of Hydrology*, **1** (**2**).

Khedr, S., Shouman, M., Fathy, N., & Attia, A. (2014). Effect of physical and chemical activation on the removal of hexavalent chromium ions using palm tree branches. *International Scholarly Research Notices*, *2014*.

Kopsidas, O. N. (2016). Scale up of adsorption in fixed-bed column systems. *Research Gate, pp1-109 http://researchgate. net/publication/322223640*.

Langmuir, I. (1916). The constitution and fundamental properties of solids and liquids. Part I. Solids. *Journal of the American Chemical Society*, **38** (**11**), 2221–2295.

Latour, R. A. (2015). The Langmuir isotherm: A commonly applied but misleading approach for the analysis of protein adsorption behavior. *Journal of Biomedical Materials Research Part A*, **103** (**3**), 949–958.

Liu, Z., Sun, Y., Xu, X., Qu, J., & Qu, B. (2020). Adsorption of Hg (II) in an Aqueous Solution by Activated Carbon Prepared from Rice Husk Using KOH Activation. *ACS omega*, **5** (**45**), 29231-29242.

Malakootian, M., Nouri, J., & Hossaini, H. (2009). Removal of heavy metals from paint industry's wastewater using Leca as an available adsorbent. *International Journal of Environmental Science & Technology*, **6** (**2**), 183-190.

Marsh, H., & Rodríguez-Reinoso, F. (2006). Characterization of Activated Carbon. In *Activated Carbon* (pp. 143–242). Elsevier.

Mckay, G. (1996). Use of Adsorbents for the Removal of Pollutants from Wastewater. CRC, Press. *Inc., USA*.

Moreno-Piraján, J. C., Rangel, D., Amaya, B., Vargas, E. M., & Giraldo, L. (2008). Design and Construction of Equipment to Make Adsorption at Pilot Plant Scale of Heavy Metals. In *Z. Naturforsch* (Vol. 63).

Nassar, M. M., Awida, K. T., Ebrahiem, E. E., Magdy, Y. H., & Mehaedi, M. H. (2003). Fixed-bed adsorption for the removal of iron and manganese onto palm fruit bunch and maize cob. *Adsorption Science & Technology*, **21** (**2**), 161-175.

Nwabanne, J. T., & Igbokwe, P. K. (2012). Comparative Study of Lead (II) Removal from Aqueous Solution Using Different Adsorbents. In *International Journal of Engineering Research and Applications (IJERA)* (Vol. 2)

Oluyemi, E., Adeyemi, A. F., & Oluremi, O. I. (2012). *Removal Of Pb2+ And Cd2+ Ions From Wastewaters Using Palm Kernel Shell Charcoal (PKSC)*.

Onundi, Y. B., Mamun, A. A., al Khatib, M. F., & Ahmed, Y. M. (2010). Adsorption of copper, nickel, and lead ions from synthetic semiconductor industrial wastewater by palm shell activated carbon. *International Journal of Environmental Science and Technology*, **7** (**4**), 751–758.

Opoku, B. K., Friday, J. O., Kofi, E. D., & Osa, E. B. (2020). Adsorption of Heavy Metals Contaminants in Used Lubricating Oil Using Palm Kernel and Coconut Shells Activated Carbons. *American Journal of Chemical Engineering*, **8** (**1**), 11-18.

Patel, H. (2019). Fixed-bed column adsorption study: a comprehensive review. *Applied Water Science*, **9** (**3**).

Patel, H. (2020). Batch and continuous fixed bed adsorption of heavy metals removal using activated charcoal from neem (Azadirachta indica) leaf powder. *Scientific Reports*, **10** (**1**), 1-12.

Rashidi, N. A., & Yusup, S. (2019). Production of palm kernel shell-based activated carbon by direct physical activation for carbon dioxide adsorption. *Environmental Science and Pollution Research*, **26** (**33**), 33732-33746.

Ronda, A., Martín-Lara, M. A., Osegueda, O., Castillo, V., & Blázquez, G. (2018). Scale-up of a packed bed column for wastewater treatment. *Water Science and Technology*, **77** (**5**), 1386-1396.

Rugayah, A. F., Astimar, A. A., & Norzita, N. (2014). Preparation and characterization of activated carbon from palm kernel shell by physical activation with steam. *Journal of Oil Palm Research*, **26** (**3**), 251-264.

Sabzehmeidani, M. M., Mahnaee, S., Ghaedi, M., Heidari, H., & Roy, V. A. (2021). Carbon based materials: a review of adsorbents for inorganic and organic compounds. *Materials Advances*, **2** (**2**), 598-627.

Saka, C., Şahin, Ö., & Küçük, M. M. (2012). Applications on agricultural and forest waste adsorbents for the removal of lead (II) from contaminated waters. In *International Journal of Environmental Science and Technology* (Vol. 9, Issue 2, pp. 379–394). Springer.

Saleem, J., Shahid, U. bin, Hijab, M., Mackey, H., & McKay, G. (2019). Production and applications of activated carbons as adsorbents from olive stones. In *Biomass Conversion and Biorefinery* (Vol. 9, Issue 4, pp. 775–802). Springer Verlag.

Sarici-Özdemir, Ç., and Önal, Y. (2014). Error analysis studies of dye adsorption onto activated carbon from aqueous solutions. *Particulate Science and Technology*, **32** (**1**), 20-27.

Setiabudi, H. D., Jusoh, R., Suhaimi, S. F. R. M., & Masrur, S. F. (2016). Adsorption of methylene blue onto oil palm (Elaeis guineensis) leaves: Process optimization, isotherm, kinetics, and thermodynamic studies. *Journal of the Taiwan Institute of Chemical Engineers*, **63**, 363–370.

Shi, Q., Sterbinsky, G. E., Prigiobbe, V., & Meng, X. (2018). Mechanistic study of lead adsorption on activated carbon. *Langmuir*, **34** (**45**), 13565-13573.

Sizirici, B., & Yildiz, I. (2020). Simultaneous removal of organics and metals in fixed bed using gravel and iron oxide coated gravel. *Results in Engineering*, *5*, 100093.

Sulaiman, F., Abdullah, N., Gerhauser, H., & Shariff, A. (2011). An outlook of Malaysian energy, oil palm industry and its utilization of wastes as useful resources. In *Biomass and Bioenergy*, **35** (**9**), 3775–3786.

Tien, C. (2019). Adsorbate Uptake and Equations Describing Adsorption Processes. In *Introduction to Adsorption* (pp. 87–118). Elsevier.

ul Haq, A., Saeed, M., Anjum, S., Bokhari, T. H., Usman, M., & Tubbsum, S. (2017). Evaluation of sorption mechanism of Pb (II) and Ni (II) onto pea (Pisum sativum) peels. *Journal of Oleo Science*, **66** (**7**), 735-743.

Ulfah, M., Raharjo, S., Hastuti, P., & Darmadji, P. (2019). The influence of textural and chemical properties of palm kernel shell activated carbon on the adsorption capacity and desorption efficiency of β-carotene in a model system. *International Food Research Journal*, **26** (**1**).

Wang, J., & Guo, X. (2020). Adsorption isotherm models: Classification, physical meaning, application and solving method. In *Chemosphere* (Vol. 258). Elsevier Ltd.

Wang, L., Shi, C., Pan, L., Zhang, X., & Zou, J. J. (2020). Rational design, synthesis, adsorption principles and applications of metal oxide adsorbents: A review. In *Nanoscale* (Vol. 12, Issue 8, pp. 4790–4815). Royal Society of Chemistry.

Wilson, E. J., & Geankoplis, C. J. (1966). Liquid mass transfer at very low Reynolds numbers in packed beds. *Industrial and Engineering Chemistry Fundamentals*, **5** (**1**), 9–14.

Yahya, M. D., Abubakar, H., Obayomi, K. S., Iyaka, Y. A., & Suleiman, B. (2020). Simultaneous and continuous biosorption of Cr and Cu (II) ions from industrial tannery effluent using almond shell in a fixed bed column. *Results in Engineering*, **6**, 100113.

Yi, Z. J., Yao, J., Chen, H. L., Wang, F., Liu, X., & Xu, J. S. (2016). Equilibrium and kinetic studies on adsorption of Pb(II) by activated palm kernel husk carbon. *Desalination and Water Treatment*, **57** (**16**), 7245–7253.